

# DEVELOPMENT OF CLOUD MASK PRODUCT USING HIMAWARI-8/AHI “JAPAN AREA” DATA

Shin Akatsuka<sup>1</sup>, Masayuki Matsuoka<sup>2</sup>, Kei Oyoshi<sup>3</sup>, Wataru Takeuchi<sup>4</sup> and Masataka Takagi<sup>5</sup>

<sup>1</sup> Kochi University of Technology, Kochi, Japan,

Email: akatsuka.shin@kochi-tech.ac.jp

<sup>2</sup> Kochi University, Kochi, Japan

Email: msykmto@kochi-u.ac.jp

<sup>3</sup> Japan Aerospace Exploration Agency, Ibaraki, Japan,

E-mail: ohyoshi.kei@jaxa.jp

<sup>4</sup> The University of Tokyo, Tokyo, Japan,

E-mail: wataru@iis.u-tokyo.ac.jp

<sup>5</sup> Kochi University of Technology, Kochi, Japan,

E-mail: takagi.masataka@kochi-tech.ac.jp

**KEY WORDS:** threshold tests, cloud detection, geostationary satellite.

**ABSTRACT:** Himawari-8 is the new Japanese geostationary satellite, which was launched on October 7<sup>th</sup>, 2014. Then the operation started on July 7<sup>th</sup>, 2015. Himawari-8 carries the Advanced Himawari Imager (AHI). Since the sensor specifications of AHI have been improved, Himawari-8/AHI can expect to be utilized not only for the meteorological monitoring, but also the environmental monitoring of land surface. In order to obtain accurate land surface parameters using satellite data, the discrimination of the cloud-contaminated pixels from cloud-free pixels is required. This study demonstrates the cloud mask production method for Himawari-8/AHI “Japan Area” data in summer and winter season. This method is based on multiple threshold tests and refers to a neutral cloud detection algorithm, which is not biased to either clear or cloudy. The algorithm is based on CLOUDIA, which is the cloud screening algorithm for GOSAT/CAI, and it is mainly composed of three parts; Reflectance tests, Brightness Temperature tests, and Integration of these tests. The cloud mask products were validated using the cloud amount data of Japan Meteorological Agency, which is ground observation data. The result showed in summer was 85.7%, and that in winter was 81.6%. However, it was revealed that the cloud detection method of this study tends to identify clear pixels as cloudy especially in winter.

## 1. INTRODUCTION

Himawari-8 is the new Japanese geostationary satellite, which was launched on October 7<sup>th</sup>, 2014 (Imai and Yoshida, 2016). Then the operation started on July 7<sup>th</sup>, 2015. Himawari-8 carries the Advanced Himawari Imager (AHI). The AHI is greatly improved over past imagers in terms of its number of bands and its temporal/special resolution (Bessho et al. 2016). Since the sensor specifications of AHI have been improved, Himawari-8/AHI can expect to be utilized not only for the meteorological monitoring, but also the environmental monitoring of land surface (Matsuoka *et al.*, 2015). In order to obtain accurate land surface parameters using satellite data, the discrimination of the cloud-contaminated pixels from cloud-free pixels is required. The purpose of this study is to develop the cloud mask production method for Himawari-8/AHI “Japan Area” data in summer and winter season.

## 2. METHODOLOGY

### 2.1 Data description

**Himawari-8/AHI “Japan Area” Data:** We used Himawari-8/AHI “Japan Area” data every hour from August 9 to 15, 2015 and from January 23 to 29, 2016. The AHI is an optical sensor with 16 spectral bands ranging from the visible to thermal infrared wave regions. The specifications of the AHI are shown in Table 1 (Japan Meteorological Agency, 2015). The AHI has five observation areas: Full Disk, Japan Area, Target Area, and two Landmark areas. The scanning area of “Japan Area” is Japan and the surrounding area, and AHI observes the area every 2.5-minute (Meteorological Satellite Center, 2016). The Himawari-8/AHI “Japan Area” data were downloaded from the National Institute of Information and Communications Technology (NICT) Science Cloud, and were preprocessed, such as radiometric correction and geometric transformation, by reference to the sample program offered by Meteorological Satellite Center (MSC) of Japan Meteorological Agency (JMA) (Matsuoka *et al.*, 2015).

Table 1. Specifications of Himawari-8/AHI

| Band |     | CW*<br>[ $\mu\text{m}$ ] | SR**<br>[km] | Band |      | CR*<br>[ $\mu\text{m}$ ] | SR**<br>[km] |
|------|-----|--------------------------|--------------|------|------|--------------------------|--------------|
| B01  | VIR | 0.47                     | 1.0          | B09  | IR   | 6.9                      | 2.0          |
| B02  |     | 0.51                     | 1.0          | B10  |      | 7.3                      | 2.0          |
| B03  |     | 0.64                     | 0.5          | B11  |      | 8.6                      | 2.0          |
| B04  | NIR | 0.86                     | 1.0          | B12  |      | 9.6                      | 2.0          |
| B05  |     | 1.6                      | 2.0          | B13  |      | 10.4                     | 2.0          |
| B06  |     | 2.3                      | 2.0          | B14  |      | 11.2                     | 2.0          |
| B07  | IR  | 3.9                      | 2.0          | B15  |      | 12.4                     | 2.0          |
| B08  |     | 6.2                      | 2.0          | B16  | 13.3 | 2.0                      |              |

\* CR : Central wave length

\*\* SR : Spatial resolution at sub satellite point

**Cloud amount data:** We used cloud amount data of JMA for accuracy evaluation of Himawari-8 cloud mask product. JMA visually observe the cloud amount every three hours at 60 meteorologically observation stations in Japan (Japan Meteorological Agency, 2016). The cloud amount means the fraction of clouds over the whole sky area. The data is expressed as an integer value from zero to ten. A zero means the cloudless and a ten means the completely overcast.

## 2.2 Cloud detection algorithm

The cloud detection algorithms are generally based on the assumption that the temperature of clouds is colder than that of the earth's surface and the reflectance of clouds is larger than that of the earth's surface. A threshold test uses these cloud properties to discriminate the cloud-contaminated pixels from cloud-free pixels by comparing a measured pixel value to the threshold value pixel-by-pixel. However, it is difficult to identify a pixel with a value around the threshold as either clear or cloudy (Ishida and Nakajima, 2009). Therefore, several cloud detection methods are designed to bias the discrimination by identifying the ambiguous pixels as cloudy or clear (Ishida and Nakajima, 2009), depending on the purpose of the observation to exclude ambiguous pixels.

The method of this study is based on multiple threshold tests and refers to a neutral cloud detection algorithm, which is not biased to either clear or cloudy (Ishida and Nakajima, 2009). The algorithm is based on CLOUDIA, which is the cloud screening algorithm for GOSAT/CAI, and it is mainly composed of four parts; Snow area detection, Reflectance tests, Brightness Temperature tests, and Integration of these tests. Table 1 shows the flow of the cloud detection algorithms.

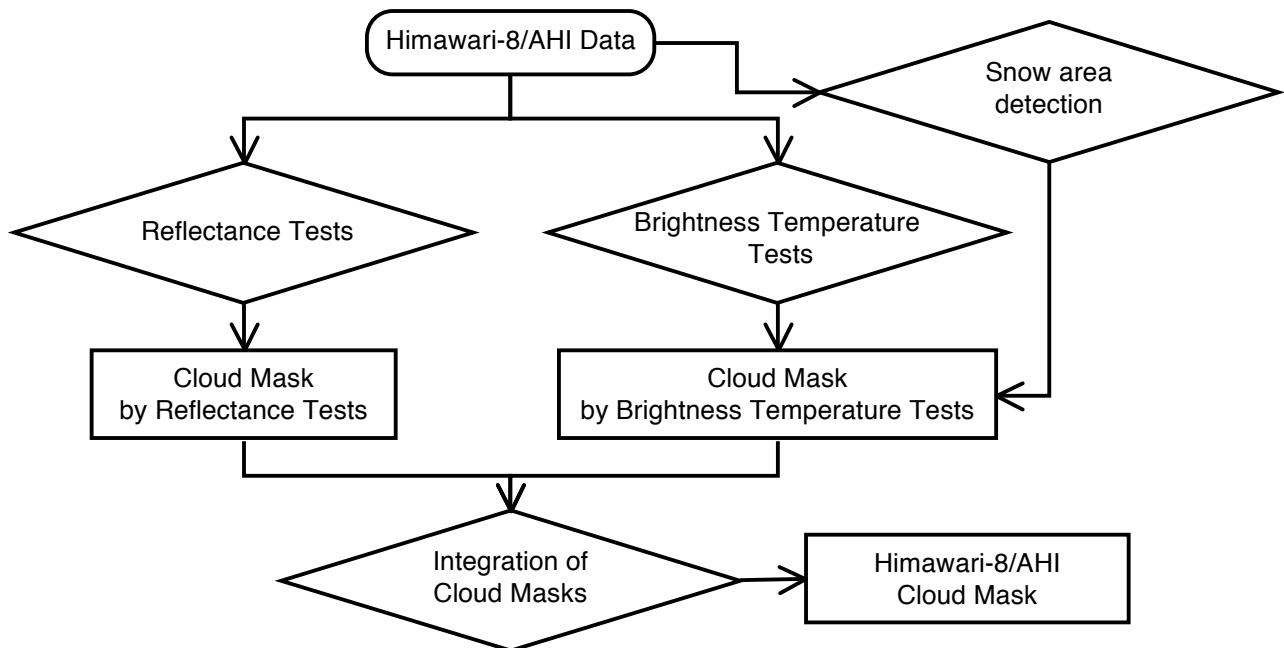


Table 1. Flow of the cloud detection algorithm

**Snow area detection:** It can be difficult to distinguish clouds from clear-sky over snow because, in general, snow have a similar observation values as clouds. Therefore, snow-covered area under clear-sky are necessary to be identified before cloud detection. In this study, Normalized Differential Snow Index (NDSI) tests were used for identifying snow-covered area under clear-sky. A pixel is flagged as being snow-contaminated if all the following conditions hold true.

$$\frac{Band5_{cl} - Band3_{cl}}{Band5_{cl} + Band3_{cl}} \geq NDSI_{threshold,cl} \quad (1)$$

$$\frac{Band5_{ob} - Band3_{ob}}{Band5_{ob} + Band3_{ob}} \geq NDSI_{threshold,ob} \quad (2)$$

where  $NDSI_{threshold}$  is pre-defined threshold,  $BandX_{ob}$  ( $X=3,5$ ) is the observed reflectance is the reflectance, and  $BandX_{cl}$  ( $X=3,5$ ) is the reflectance of  $BandX$  composite map for 30 days before the date of satellite data for cloud detection. The snow-covered areas are combined with the cloud mask by brightness temperature test.

**Reflectance Tests:** The reflectance tests are generally based on the assumption that the reflectance of clouds is larger than that of the earth's surface. The reflectance tests comprise three tests: Single Reflectance Test, NDVI Test, and VIR/NIR ratio Test. The VIR/NIR ratio Test is applied to only daytime and twilight pixels, which are defined by the solar zenith angle. A pixel is flagged as being cloud-contaminated if the following conditions hold true.

(G1.1) Single Reflectance Test

$$\text{Land : } Band3_{ob} - Band3_{cl} > \Delta R_{Band3}^{land} \quad (3)$$

$$\text{Sea : } Band4_{ob} - Band4_{cl} > \Delta R_{Band4}^{sea} \quad (4)$$

(G1.2) NDVI Test

$$NDVI_{ob} > NDVI_{threshold} \quad (5)$$

(G1.3) VIR/NIR ratio Test

$$\text{Land : } \frac{Band4_{ob}}{Band3_{ob}} \geq \Delta R_{B4/B3}^{land} \quad (6)$$

$$\text{Sea : } \frac{Band4_{ob}}{Band3_{ob}} \geq \Delta R_{B4/B3}^{sea} \quad (7)$$

where  $\Delta R$  and  $NDVI_{threshold}$  are pre-defined thresholds,  $BandX_{ob}$  ( $X=3,4$ ) is the observed reflectance is the reflectance, and  $BandX_{cl}$  ( $X=3,4$ ) is the reflectance of  $BandX$  composite map for 30 days before the date of satellite data for cloud detection. These threshold values were determined by reference the previous studies and visual inspection of satellite data.

The reflectance tests has a possibility of incorrectly identifying clear sky areas as cloudy if the surface under the clear sky is confusing, such as desert and thick forest (Ishida and Nakajima, 2009). In other words, the reflectance tests tend to bias the discrimination by identifying the ambiguous pixels as cloudy (Ishida and Nakajima, 2009). Therefore, the final discrimination is carried out by the following equation. This equation means that the pixels are finally identified as cloudy ( $G_I=0$ ) only if the pixels are identified as cloudy by all the reflectance tests.

$$G_I = 1 - (1 - F_1) * (1 - F_2) * (1 - F_3) \quad (8)$$

where  $F_k$  ( $k = 1, \sim, 3$ ) is the flag of the  $k$ th threshold test:  $F_k = 1$  (clear),  $F_k = 0$  (cloudy).

**Brightness Temperature Tests:** The brightness temperature tests are generally based on the assumption that the temperature of clouds is colder than that of the earth's surface. A pixel is flagged as being cloud-contaminated if the following conditions hold true.

(G2.1) Temperature Test

$$Band13_{cl} \leq T_{Band13cl} \quad (9)$$

$$Band14_{ob} \leq T_{Band14ob} \quad (10)$$

$$Band9_{ob} \leq T_{Band9ob} \quad (11)$$

(G2.2) Gross Test

$$Band13_{ob} - Band13_{cl} < \Delta T_{Band13} \quad (12)$$

(G2.3) Thin Cirrus Test

$$Band14_{ob} < T_{Band14ob} \quad \text{or,} \quad (Band14_{ob} - Band15_{ob}) - (Band14_{cl} - Band15_{cl}) > \Delta T_{Band14,15} \quad (13)$$

(G2.4) Fog/Low Cloud Test

$$Band14_{ob} < T_{Band14ob} \quad \text{or,} \quad (Band14_{ob} - Band11_{ob}) - (Band14_{cl} - Band11_{cl}) > \Delta T_{Band14,11} \quad (14)$$

$$Band14_{ob} < T_{Band14ob} \quad \text{or,} \quad (Band14_{ob} - Band7_{ob}) - (Band14_{cl} - Band7_{cl}) > \Delta T_{Band14,7} \quad (15)$$

where  $T$ ,  $\Delta T$  and  $NDVI_{threshold}$  are pre-defined thresholds,  $BandX_{ob}$  ( $X=7,11,13,14,15$ ) is the observed reflectance is the reflectance, and  $BandX_{cl}$  ( $X=7,11,13,14,15$ ) is the reflectance of  $BandX$  composite map for 30 days before the date of satellite data for cloud detection. These threshold values were determined by reference the previous studies and visual inspection of satellite data.

The brightness temperature tests have a possibility of falsely identifying cloudy pixels as clear (Ishida and Nakajima, 2009). In other words, the reflectance tests tend to bias the discrimination by identifying the ambiguous pixels as clear (Ishida and Nakajima, 2009). Therefore, the final discrimination is carried out by the following equation. This equation means that the pixel are finally identified as cloudy ( $G_2=0$ ) at least one of the brightness temperature tests result in 0.

$$G_2 = F_4 * F_5 * F_6 * F_7 * F_8 * F_9 * F_{10} \quad (16)$$

where  $F_k$  ( $k = 5, \sim, 10$ ) is the flag of the  $k$ th threshold test:  $F_k = 1$  (clear),  $F_k = 0$  (cloudy).

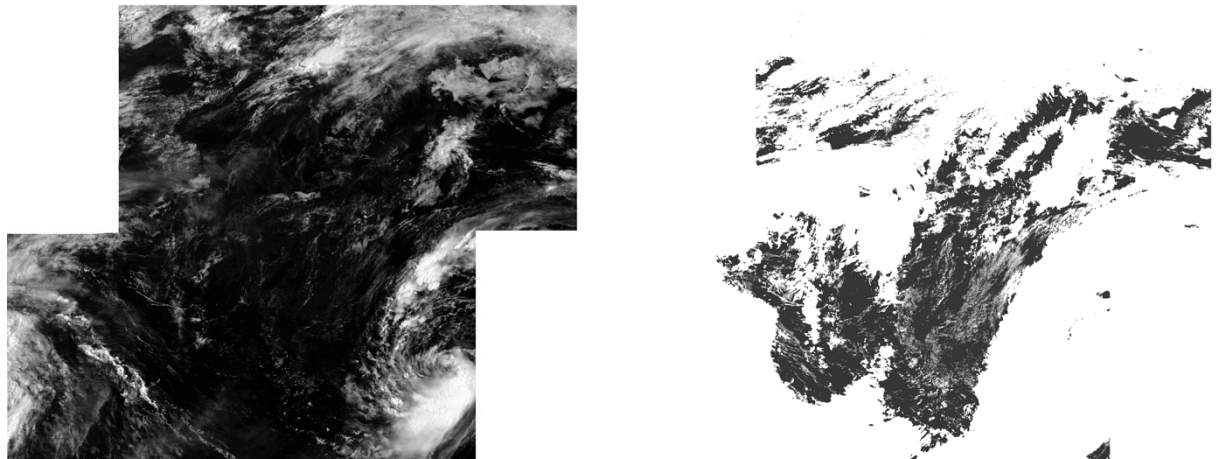
**Integration of these tests:** The results of reflectance tests and brightness temperature tests are integrated by the following equation. This equation means that the pixels identified as cloudy by either reflectance tests or brightness temperature tests were finally determined as cloud-contaminated pixels.

$$Q = G_1 * G_2 \quad (17)$$

The value of  $Q$  is either 0 or 1. A zero means cloudy and a one means clear. The final Himawari-8 cloud mask product is based on the flag by the  $Q$  value. Therefore, Himawari-8 cloud mask product of this study comprises two flags: clear and cloudy.

### 3. RESULTS AND DISCUSSION

The Results of cloud detection in summer and winter were shown in Figure 2 and Figure 3, respectively. The threshold values of all threshold tests were determined by reference the previous studies and visual inspection of satellite data (Ishida and Nakajima, 2009; Hocking *et al.*, 2011). By visual interpretation from these figures, the cloud detection method of this study tends to identify clear pixels as cloudy.



(a) Band03 image

(b) Himawari-8 cloud mask

Figure 2. Result of cloud detection at 0000UTC 09 August, 2015.

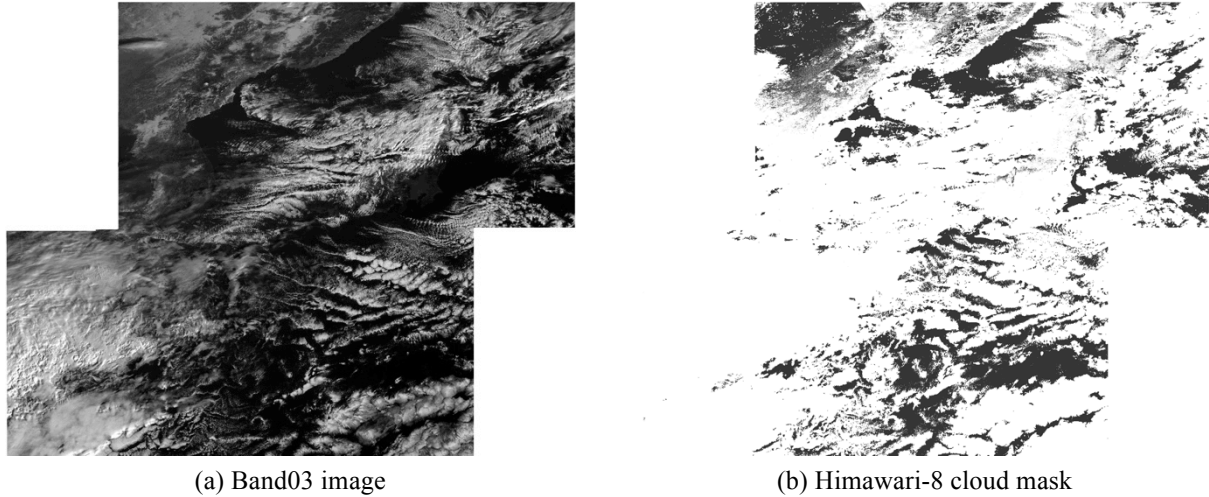


Figure 3. Result of cloud detection at 0000UTC 27 January, 2016.

We evaluated the accuracy of Himawari-8 cloud mask product using the cloud amount data of JMA. Himawari-8 cloud mask product of this study comprises two flags: clear and cloudy, whereas the cloud amount data of JMA is expressed as 11 levels from zero to ten. A zero means the cloudless and a ten means the completely overcast. Therefore, the cloud amount data of JMA are classified into two categories (i.e. clear and cloudy). In this study, the cloud amount 0 and 1 are defined as clear, and others are defined as cloudy. Then the agreement rate of clear/cloudy among them is evaluated by overall accuracy using confusion matrixes.

Table 2 and Table 3 show the results of accuracy evaluation in summer and winter season respectively. These results showed the overall accuracy in summer was 85.7% and that in winter was 81.6 %. In winter, the accuracy of cloud detection was reduced. In addition, Table 3 also shows that this method detects cloudy area excessively in winter. One reason why is that the surface temperature under clear-sky is lower in winter and the temperature difference between the cloud-contaminated pixels and cloud-free pixels is small.

Table 2. Results of accuracy evaluation in summer season

|                                     |                        | JAM Observation Data              |                                   |      |                    |
|-------------------------------------|------------------------|-----------------------------------|-----------------------------------|------|--------------------|
|                                     |                        | Clear<br>(Cloud amount : 0 and 1) | Cloudy<br>(Cloud amount : 2 - 10) | SUM  | User's<br>Accuracy |
| Himawari-8<br>cloud mask<br>product | Clear                  | 82                                | 269                               | 351  | 23.4 %             |
|                                     | Cloudy                 | 68                                | 1933                              | 2001 | 96.6 %             |
|                                     | SUM                    | 150                               | 2202                              | 2352 |                    |
|                                     | Producer's<br>Accuracy | 54.7 %                            | 87.8 %                            |      | 85.7 %             |

Table 3. Results of accuracy evaluation in winter season

|                                     |                        | JAM Observation Data              |                                   |      |                    |
|-------------------------------------|------------------------|-----------------------------------|-----------------------------------|------|--------------------|
|                                     |                        | Clear<br>(Cloud amount : 0 and 1) | Cloudy<br>(Cloud amount : 2 - 10) | SUM  | User's<br>Accuracy |
| Himawari-8<br>cloud mask<br>product | Clear                  | 73                                | 169                               | 242  | 30.2 %             |
|                                     | Cloudy                 | 254                               | 1807                              | 2061 | 87.7 %             |
|                                     | SUM                    | 327                               | 1976                              | 2303 |                    |
|                                     | Producer's<br>Accuracy | 22.3 %                            | 91.4 %                            |      | 81.6 %             |

#### 4. CONCLUSION

In this study, we developed the cloud mask production method for Himawari-8/AHI "Japan Area" data in summer and winter season. This method is based on multiple threshold tests and refers to a neutral cloud detection algorithm,

which is not biased to either clear or cloudy. The accuracy of the cloud detection was evaluated by the agreement rate between Himawari-8 cloud mask product and cloud amount data of JMA. The overall accuracy was calculated using confusion matrixes. The overall accuracy in summer was 85.7%, and that in winter was 81.6%. However, by visual interpretation, it was revealed that the cloud detection method of this study tends to identify clear pixels as cloudy especially in winter. In other words, this method detects cloudy area excessively. Because the surface temperature under clear-sky is lower and the temperature difference between the cloud-contaminated pixels and cloud-free pixels is small in winter, cloudy area as excessively detected and the accuracy of cloud detection was reduced in winter. Therefore, we need to review values of pre-defined threshold for multiple threshold tests, especially for the brightness temperature tests.

## ACKNOWLEDGEMENT

AHI data were provided by the Japan Meteorological Agency, via the NICT Science Cloud at the National Institute of Information and Communications Technology, as collaborative research. This research was supported by Ministry of Education, Culture, Sports, Science and Technology, Japan.

## REFERENCES

- Bessho, K., Date, K., Hayashi, M., Ikeda, A., Imai, T., Inoue, H., Kumagai, Y., Miyakawa, T., Murata, H., Ohno, T., Okuyama, A., Oyama, R., Sasaki, Y., Shimazu, Y., Shimoji, K., Sumida, Y., Suzuki, M., Taniguchi, H., Tsuchiyama, H., Uesawa, D., Yokota, H. and Yoshida, R., 2016. An introduction to Himawari-8/9 - Japan's new-generation geostationary meteorological satellite. *J. Meteor. Soc. Japan*. 94.
- Hocking, J., Francis, P.N. and Saunders, R., 2011, Cloud detection in Meteosat Second Generation imagery at the Met Office. *Meteorological Applications*, vol.18, pp.307-323.
- Imai, T. and Yoshida, R., 2016, Algorithm Theoretical Basis for Himawari-8 Cloud Mask Product. *Meteorological Satellite Center Technical Note*, No.61.
- Ishida, H. and Nakajima, Y.T., 2009. Development of an unbiased cloud detection algorithm for a spaceborne multispectral imager. *Journal of Geophysical Research*, vol. 114.
- Matsuoka, M., Honda, R., Nonomura, A., Moriya, H., Akatsuka, S., Yoshioka, H. and Takagi, M, 2015. A Method to Improve Geometric Accuracy of Himawari-8/AHI "Japan Area" Data. *Journal of the Japan Society of Photogrammetry and Remote Sensing*, vol. 54, No.6, pp.280-289.
- Japan Meteorological Agency, 2015. Himawari-8/9 Himawari Standard Data User's Guide (ver. 1.1). Retrieved September 10, 2016, [http://www.data.jma.go.jp/mscweb/en/himawari89/space\\_segment/hsd\\_sample/HS\\_D\\_users\\_guide\\_en\\_v11.pdf](http://www.data.jma.go.jp/mscweb/en/himawari89/space_segment/hsd_sample/HS_D_users_guide_en_v11.pdf)
- Japan Meteorological Agency. Retrieved April 6, 2016, <http://www.data.jma.go.jp/obd/stats/etrn/index.php>
- Wildt, M.R., 2006. Improved Methods for Snow-Cloud Separation Using Multi-temporal Meteosat-8 SEVIRI Imagery. *COSMO Newsletter No.6*, pp.11-22. Retrieved September 10, 2016, from [http://www2.cosmo-model.org/content/model/documentation/newsLetters/newsLetter06/cnl6\\_dewildt.pdf](http://www2.cosmo-model.org/content/model/documentation/newsLetters/newsLetter06/cnl6_dewildt.pdf)
- Meteorological Satellite Center, Japan Meteorological Agency. Retrieved September 10, 2016, from: [http://www.data.jma.go.jp/mscweb/en/himawari89/space\\_segment/spsg\\_ahi.html](http://www.data.jma.go.jp/mscweb/en/himawari89/space_segment/spsg_ahi.html)